Appendix B

Bose et al., Characterization and molecular modeling of a highly stable anti-Hepatitis B surface antigen scFv, Molecular Immunology, 40, pp617-31, 2003

Available online at www.sciencedirect.com
SCIENCE DIRECT
PERGAMON
Molecular Immunology 40 (2003) 617–631
Molecular Immunology
www.elsevier.com/locate/molimm

Characterization and molecular modeling of a highly stable anti-Hepatitis B surface antigen scFv

Biplab Bose [a], Dipti A. Chugh [b], Mrinalini Kala [a,1], Subrat K. Acharya [c], Navin Khanna [b], Subrata Sinha [a,*]

[a] *Department of Biochemistry, All India Institute of Medical Sciences, Ansari Nagar, New Delhi, PIN-110029, India*
[b] *International Center for Genetic Engineering and Biotechnology, New Delhi, India*
[c] *Department of Gastroenterology, All India Institute of Medical Sciences, New Delhi, India*

Received 3 April 2003; received in revised form 20 May 2003; accepted 11 July 2003

Abstract

We raised a mouse monoclonal antibody (5S) against the 'a' epitope of the Hepatitis B surface antigen (HBsAg) by selecting for binding of the hybridoma supernatant in conditions that usually destabilize protein–protein interactions. This antibody, which was protective in an in vitro assay, had a high affinity with a relative dissociation constant in the nanomolar range. It also displayed stable binding to antigen in conditions that usually destabilize antigen–antibody interactions, like 30% DMSO, 8 M urea, 4 M NaCl, 1M guanidium HCl and extremes of pH. The variable regions of the antibody were cloned and expressed as an single chain variable fragment (scFv) (A5). A5 had a relative affinity comparable to the mouse monoclonal and showed antigen binding in presence of 20% DMSO, 8 M urea and 3 M NaCl. It bound the antigen in the pH range of 6–8, though its tolerance for guanidium HCl was reduced. Sequence analysis demonstrated a significant increase in the frequency of somatic replacement mutations in CDRs over framework regions in the light but not in the heavy chain. A comparison of the molecular models of the variable regions of the 5S antibody and its germ-line precurser revealed that critical mutations in the heavy and light chains interface resulted in better inter-chain packing and in the movement of CDR H3 and CDR L1 from their germline positions, which may be important for better antigen binding. In addition to providing a reagent for neutralizing for the virus, such an antibody provides a model for the evolution of stable high affinity interaction during antibody maturation.

Keywords: Anti-HBs antibody; Recombinant antibody; Protein–protein interactions; Somatic mutations; Molecular modeling

1. Introduction

Hepatitis B infection is a global public health problem with an estimated 300 million carriers world wide, of which over 250,000 die annually from Hepatitis B associated liver diseases. The major humoral response to the Hepatitis B virus is mounted against the Hepatitis B surface antigen (HBsAg) with the appearance of anti-HBs antibody in patient's blood after about 6 months of infection. Following natural infection with HBV or after immunization with HBsAg, protective immunity correlates with induction of antibodies against the group specific 'a' determinant, which is present in all serotypes (McAuliffe et al., 1980). However, neutralizing epitopes are also present in pre-S1 and -S2 regions (Sureau et al., 1992). The 'a' determinant (amino acids 124–147) is now considered to be a part of a large antigenic area called the major hydrophilic region (MHR) (Milich et al., 1997). Neutralizing activity of anti-HBs antibody against the 'a' determinant has also been demonstrated with an in vitro system (Shearer et al., 1998). Although there is a common notion that in vitro binding to the virion does not always guaranty neutralization, there is growing evidence that neutralization is directly correlated to occupancy of sites on the virion (Burton et al., 2000; Klasse and Sattentau, 2002). A stable high affinity antigen–antibody interaction has been shown to be an attribute of neutralizing antibodies (Maynard et al., 2002; Willuda et al., 1999). An antibody providing high affinity for the antigen in an in vitro system may also neutralize the virus through inhibition of virus attachment and early entry functions (Klasse and Sattentau, 2002). It has been shown that $F(ab)_2$ fragments derived from Hepatitis B immune globulin can prevent perinatal transmission

* Corresponding author. Tel.: +91-11-659-3314; fax: +91-11-2658-8663/8641.
E-mail address: sub_sinha@hotmail.com (S. Sinha).
[1] Present address: Department of Pulmonary and Critical Care Medicine, University of California, San Francisco, USA.

0161-5890/$ – see front matter © 2003 Elsevier Ltd. All rights reserved.
doi:10.1016/j.molimm.2003.07.002

of Hepatitis B virus carrier state in neonates (Tada et al., 1982).

In this paper, we report the characterization of 5S, an anti-HBs mouse monoclonal of isotype IgG1 that binds to the S domain of the antigen, and its corresponding single chain variable fragment (scFv). The hybridoma was selected by assaying for supernatant binding in the presence of 3 M KCNS in order to ensure stable antigen–antibody interaction. This monoclonal tested positive in an in vitro test for sero-conversion and protective antibodies. 5S has a very high affinity for the antigen and the binding is highly stable in presence of different agents that destabilize antigen–antibody interactions, like urea, DMSO, high salt and extreme pH. The recombinant scFv fragment (A5) also shows very high affinity for the antigen and also retains most of its antigen binding in the presence of different destabilizing agents. We further report the statistical analysis of the mutations, which have taken place in the process of antigen driven somatic hypermutation during repeated immunization. Also, based on molecular modeling of the antibody and its germline counterpart, we have attempted to delineate the importance of these somatic mutations in the mature antibody for stable, high affinity antigen binding.

2. Materials and methods

2.1. Materials

Phage display vector pHEN1 (kindly provided by Dr. Greg Winter, MRC, Cambridge, UK) was used for expression of recombinant antibody fragment. *Escherichia coli* strains TG1 and HB2151^{Nal} (from MRC, Cambridge) were used for expression of phage antibody and soluble scFv, respectively. Hybridoma 5S expressing antibody against HBsAg was maintained in RPMI (Sigma, USA) with 10% FCS (Sigma, USA). Shanta Biotech, India, provided purified recombinant HBsAg expressed in a *Pichia* system.

2.2. Generation of hybridoma

Six Balb/c mice were immunized with 5 μg of plasma derived HBsAg intraperitonially after emulsification with FCA. Mice were boosted twice with 1 μg of HBsAg at 1 and 4 months interval. After the third immunization, sera from individual animals were screened for the presence of protective antibodies to HBsAg. We used a commercial kit (Hepanostika anti-HBs kit from Organon Teknika, The Netherlands), for this purpose. This kit is customarily employed to asses sero-conversion in HBsAg immunized individuals. By this kit, 10 IU anti-HBs/l is generally accepted to be sufficient to indicate protective immunity against Hepatitis B virus infections (Gamelkoorn, 1991). Although this assay is not equivalent to in vitro neutralization assay, it is useful in absence of any in vitro culture system for HBV. The test is a sandwich enzyme-immuno assay. The screening protocol was as described by the manufacturer with one modification. After binding of the antibody to antigen coated on the well, a wash step of 1–3 M potassium thiocynate in phosphate buffer for 10 min was included before the addition of enzyme labeled HBsAg. The mice whose sera exhibited stable binding to HBsAg in presence of 3 M KSCN were used as a source of spleen cells for the production of hybridomas. Fusion and screening protocols were as described by Harlow and Lane (1988). Once again resultant hybridoma supernatants were screened for binding in the presence of 3 M-KSCN.

2.3. Amplification of antibody variable region genes

Total RNA was extracted from hybridoma cells using TRI reagent (Sigma, USA). cDNAs were generated by reverse transcription (Omniscript RT Kit, QIAGEN) using a primer against 3′-end conserved region of antibody variable region genes. PCR amplification of V_H and V_L was performed with degenrate primers, for 35 cycles of 94 °C for 1 min, 50 °C for 1 min and 72 °C, 2 min; followed by a final extension at 72 °C for 10 min. PCR products were eluted using a QIAquick gel extraction kit. Primers used for amplification of light chain were 5′-ATT GTG ATG ACC CAG ACT-3′ and 5′-TCG ACT TGC GGC CGC CCG TTT KAK YTC CAR CTT KGT SCC-3′. Primers utilized for PCR amplification of heavy chain were 5′-GCA ACT GCG GCC CAG CCG GCC ATG GCC GAG GTG CAG CTK CAG CTK CAG CAG-3′ and 5′-TGA RGA GAC RGT GAC TGA RGT-3′. Oligoneucleotides used for generation of the linker fragment and for joining it to the heavy and light chain were 5′-GGT GGT GGT GGG AGC GGT GGT GGC ACT GGC GGC GGC GGA TCT-3′, 5′-TCA GTC ACY GTC TCY TCA GGT GGT GGT GGG AGC-3′, and 5′-GT CTG GGT CAT CAC AAT AGA TCC GCC GCC GCC-3′.

2.4. Construction of 5S-scFv expression vector

PCR amplified V_H and V_L fragments were joined with a linker $(Gly_4Ser)_3$ by overlap PCR. In brief, a double-stranded linker fragment was constructed by PCR using the linker template and primers carrying overhangs corresponding to V_H and V_L fragments. Initial assembly of equimolar amounts of linker, V_H and V_L was done by PCR for 20 cycles at 94 °C for 1 min, 50 °C for 1 min, 72 °C for 2 min, followed by final extension of 10 min at 72 °C. The product of the initial assembly reaction was diluted 10 times and used as template for pull through PCR using primers for 5′-end of V_H and 3′-end of V_L fragment. PCR products were resolved in 1.5% agarose gel and the band for assembled scFv was eluted out using QIAquick gel extraction kit. Assembled scFv was then digested with NotI and SfiI and ligated into the phagemid vector pHEN1 (Hoogenboom and Winter, 1992), which was double digested with the same pair of restriction enzymes. TG1 cells were

transformed with the resulting phagmid pHEN1-5S-scFv in using a standard chemical transformation protocol (Sambrook and Russell, 2001) and colonies were selected for presence of insert by PCR screening and restriction digestion.

2.5. Expression of phage antibody and selection of antigen binding clones

The pHEN1 vector carrying scFv fragment was transformed into the suppressor *E. coli* strain TG1 for expression of phage antibody. Phage displaying scFv were rescued by infection with helper phage (M13-K07). After overnight growth, phage antibodies were precipitated from the media supernatant by PEG/NaCl. Precipitated phage were re-suspended in PBS and titrated out for determination of phage concentration (Barbas et al., 2001).

Selection of antigen binding clones was done over immuno-plates. Maxisorp ELISA plates were coated with HBsAg (250 ng per well) in bicarbonate buffer pH 9.5. Both coated and uncoated wells of the ELISA plate were blocked with 2% non-fat milk PBS (MPBS) at 37 °C for 2 h. Approximately 10^{10} phage in 2% MPBS were added to an uncoated well and incubated at room temperature for 1 h and unbound phage were then pipetted out and added to the antigen coated well. After incubation for 1 h at room temperature, wells were washed with 0.1% Tween-20 PBS (TPBS) and three times with PBS. Bound phage were eluted out by incubating 10 min with 100 nM glycine pH 2.5 and immediately neutralized by 1 M Tris buffer at pH 7.4. Eluted phage were passed through two more rounds of selection over coated and uncoated wells with increased number of washing with TPBS and PBS.

2.6. Identification of antigen binding clones by phage-ELISA

Phage obtained after three rounds of selections were re-infected in TG1 and amplified by standard protocol as mentioned earlier. Antigen binding clones were identified by phage-ELISA. Maxisorp ELISA plates were coated with 250 ng per well of HBsAg in bicarbonate buffer (pH 9.5). After blocking with 2% MPBS, approximately 10^{12} phage were added and incubated for 1 h at room temperature. Bound phage were detected by incubation with 1:1000 dilution of anti-M13 mouse antibody (kindly provided by Dr. Vijay Chaudhary, University of Delhi, South Campus, New Delhi, India) for 1 h at room temperature, followed by 1 h incubation with 1:2000 dilution of anti-mouse antibody–HRP conjugate. ELISA was developed by using 100 μl of 0.4 mg/ml *o*-phenylenediamine (OPD) and 0.8 μl/ml of H_2O_2 in citrate-phosphate buffer (pH 5). The same amount of a heat stable alkaline phosphatase (HSAP) binding scFv was used as negative control in phage-ELISA.

2.7. Soluble expression and immunoblot analysis of 5S-scFv

The antigen-binding clone identified by phage-ELISA was transformed in non-suppressor *E. coli* ($HB2151^{Nal}$) for soluble expression of the scFv. After 8 h of induction with 2 mM IPTG, soluble scFv was harvested from the bacterial periplasm as described by Kala et al. (2001). Periplasmic extracts from both transformed and un-transformed $HB2151^{Nal}$ cells were resolved on a 12% reducing SDS PAGE and stained with Coomassie Brilliant Blue R-250. Proteins were resolved on SDS/PAGE, blotted to nitrocellulose membrane. After blocking the membrane with 4% MPBS, the scFv was detected on the blot by incubating with anti-c-*myc* mouse antibody followed by anti-mouse HRP conjugate. The blot was developed using DAB/HRP system.

2.8. Antigen binding assay for the scFv

The binding assay for the scFv was done both by ELISA and sandwich ELISA. For direct measurement of antigen binding activity, ELISA plates were coated with 250 ng per well of antigen in bicarbonate buffer (pH 9.5). After blocking with 3% MPBS, different dilutions of periplasmic extracts of both transformed and untransformed cells were incubated for 1 h at room temperature. Bound scFv was detected with anti-c-*myc* mouse antibody, followed by anti-mouse HRP conjugate.

For sandwich ELISA, the plate was coated with 100 μl per well of 1:10 dilution of 5S hybridoma supernatant. Antigen of 250 ng per well was added to those antibody-coated wells and captured antigen was incubated with periplasmic extracts (1:20 dilution in PBS). Bound scFv was detected with anti-c-*myc* antibody followed by anti-mouse antibody-HRP conjugate.

Competitive ELISA was done to confirm that the recombinant antibody fragment binds to the same epitope as that of the mouse monoclonal. Different dilutions of periplasmic extract were added to antigen coated ELISA plate in presence of 1:1500 dilution of mouse monoclonal and allowed to compete for 1hr at room temperature. Bound mouse monoclonal was detected using anti-mouse-HRP conjugate. Periplasmic extract of untransformed HB2151 cells was used as negative control in this experiment.

Strength of binding of the recombinant antibody fragment was also assayed qualitatively by performing ELISA at different concentrations of NaCl, urea, DMSO, guanidium HCl and at different pH. 1:100 dilution of periplasmic extract was made in PBS having different concentrations of NaCl (500 mM to 4 M), urea (0.5–8 M), DMSO (0–30%), and guanidium HCl (0–4 M). Diluted periplasmic extracts were added to antigen coated ELISA plates and bound scFv was detected with anti-c-*myc* antibody. Similar experiments were performed at different pHs with phosphate

buffer at pH 6, 7.4, and 8. Carbonate buffer was used for pH 9.2, 10 and 11 and citrate buffer was used for pH 4. Similar experiments were performed with the mouse monoclonal 5S.

2.9. Determination of K_D of the scFv

Dissociation constant K_D value of HBsAg and scFv interaction was determined in solution phase by an ELISA method as described by Friguet et al. (1985). Essentially the technique involves incubation of different dilutions of antibody with different amount of antigen in solution phase for a prolonged period so that equilibrium is reached, followed by detection of unbound antibody by conventional ELISA.

Different dilutions of antigen (0.1–10 nM) were incubated with diluted periplasmic extract for 16 h at 4 °C, so that equilibrium of the antigen–antibody reaction was reached. Hundred microliters of such equilibrated solution was incubated in antigen coated ELISA plates (250 ng per well of antigen) for 20 min at room temperature to capture free scFv. Bound scFv was detected with anti-c-*myc*/anti-mouse–HRP system as described before.

2.10. Sequencing analysis and modeling of V regions

The scFv fragment present in pHEN1 phagemid vector was sequenced using dideoxy method with vector specific sequencing primers LMB3 (5′-CAG GAA ACA GCT ATG AC-3′) and pHENSEQ (5′-CTA TGC GGC CCC ATT CA-3′) in an automated sequencing machine ABI prism system, Model 377, version 2.12.

Both the heavy and light chains variable region sequences were numbered as per Kabat rule (Kabat et al., 1991). Canonical classes of each of the CDR regions were identified as per Chothia and Lesk (1987) using on line software at the web site "Antibodies—Structure and Sequence" (http://www.bioinf.org.uk/abs/). The scFv sequence was submitted to the EMBL Nucleotide Sequence Database (EMBL accession number is AJ549501) and analyzed by online V-Quest software provided by the International ImMunoGeneTics database (IMGT, http://imgt.cines.fr: 8104) for identification of germline origin of V_H/V_L regions (Lefranc, 2001). Expected numbers of replacement mutations and silent mutations in CDR and FR regions were calculated as per Bagley et al. (1994) considering a normal distribution and statistical analysis was done by chi-square test.

A tentative structure of the variable region of this antibody and its germline counterpart were generated by molecular modeling using web based antibody modeling software WAM (Whitelegg and Rees, 2000) (http://antibody.bath.ac.uk/index.html), which uses a modified form of the algorithm used in antibody modeling software AbM of Oxford Molecular. We used the 'dead end elimination' algorithm (De Maeyer et al., 2000) for side chain building and VFF screen (Dauber-Osguthorpe et al., 1988) for final screening. Once modeled automatically, we compared both the heavy and light chains with most homologous antibodies in Protein Data Base (Bernstein et al., 1977), having same loop lengths. Homology searches for nucleotide and protein sequences were done using BLAST (Altschul et al., 1990). Molecular models were viewed and analyzed using SwissPdb Viewer (Guex and Peitsch, 1997) and Accelrys ViewerLite Version 5.0.

3. Results

3.1. Generation of 5S mouse monoclonal

5S is a mouse monoclonal expressing anti-HBs IgG1. This hybridoma was generated by using a stringent screening method as described in the Section 2. Only those antibodies were selected that retained antigen binding in the presence of 3 M KSCN. This step was included first for the screening of sera of immunized animals and also for screening hybridoma supernatants. The culture supernatant of 5S hybridoma showed stable binding to HBsAg in presence of 3 M KSCN. Such a stringent procedure ensured that we had a source of very high affinity anti-HBs, which was also recognized by a commercial kit (Hepanostika anti-HBs) routinely used as a surrogate test for the evaluation of sero-conversion and evaluation of the generation of protective antibodies to hepatitis B virus infection.

3.2. Cloning of the scFv fragment in phagemid system

Variable regions of both the light and heavy chains of 5S hybridoma were amplified by RT-PCR and connected with a flexible linker to generate single chain variable fragment by overlap PCR. Phagemid vector pHEN1 was used for expression of the scFv fragment as phage antibody as well as soluble scFv in *E. coli* system. The vector provides a c-*myc* tag at the C-terminal of the scFv for easy identification of the recombinant antibody.

3.3. Selective enrichment of antigen binding clones and phage-ELISA

Although we had cloned the variable regions of a mouse monoclonal for expression of scFv, it is well known that truncation and mutations can be generated due to PCR and the cloning process. Therefore, we enriched our cloned library for functional scFvs by bio-panning over antigen coated ELISA plate. Selection was done alternatively over coated and uncoated plates. After three rounds of enrichment, selected clones were used to prepare phage antibody and antigen-binding clones were detected by phage-ELISA. Clone A5 which showed the maximum absorbance has been used for further studies.

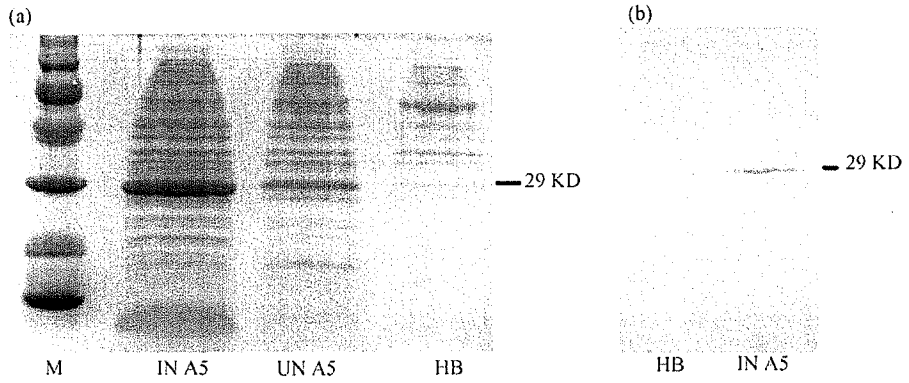

Fig. 1. SDS PAGE (a) and Western blot (b) for A5 scFv expressed in soluble form. In (a) lanes IN A5 and UN A5 are for periplasmic extract of IPTG induced A5 and uninduced A5, respectively. HB and M are for periplasmic extract of untransformed HB2151^{Nal} cells and protein marker, respectively. Periplasmic extracts were resolved in a 12% SDS page in denaturing condition and stained with Coomassie Brilliant Blue R-250. (b) Western blot for soluble A5 scFv. The scFv was detected using anti-c-*myc* antibody followed by anti-mouse HRP conjugate. Lanes HB and IN A5 are for periplasmic extract of untransformed HB2151^{Nal} and induced clone A5, respectively.

3.4. Soluble expression of anti-HBs scFv

The anti-HBs scFv clone A5 (A5 scFv) was expressed in soluble form by inducing A5 infected HB2151^{Nal} culture with 2 mM IPTG for 8 h at 30 °C. After induction, a band with molecular weight of ~29 kDa, corresponding to scFv was detected in the periplasmic extract of A5 infected HB2151^{Nal} cells (Fig. 1a). This was further confirmed by Western blot using anti-c-*myc* antibody (Fig. 1b).

3.5. Study of antigen binding activity of recombinant A5 scFv

Fig. 2 shows binding of different dilutions of unpurified A5 scFv to the recombinant antigen as detected by ELISA. As mentioned in the methods section, recombinant scFv was allowed to bind to HBsAg coated on ELISA plate and the bound scFv was detected by anti-c-*myc* antibody. Binding of A5 scFv to the antigen was further confirmed by sandwich ELISA. Sandwich ELISA was performed using the same periplasmic extract. Both the recombinant scFv and the hybridoma supernatant that was used as positive control were used at a saturating dilution and as shown in Fig. 3, both of them show comparable binding. It was further confirmed by competitive ELISA, that the recombinant scFv A5 binds to the same epitope as that of the mouse monoclonal 5S (data not shown).

3.6. Stability of antigen–antibody interactions

To study the stability of the antigen–antibody complex formed by A5 scFv and to understand the molecular forces

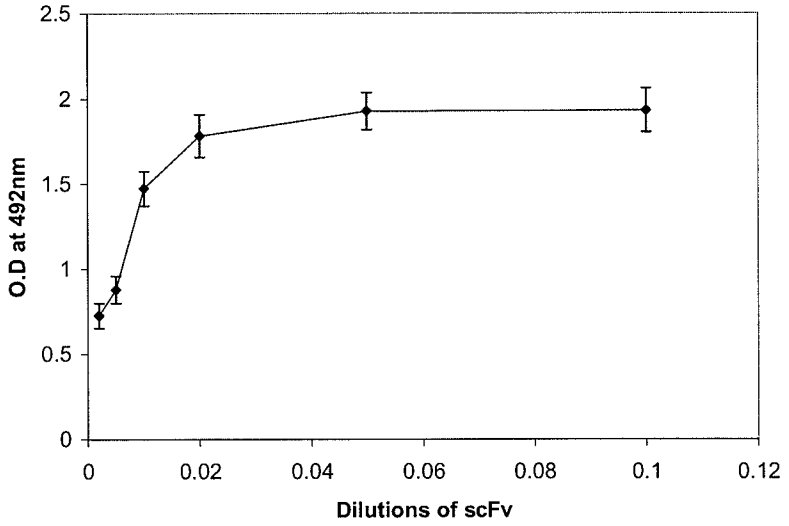

Fig. 2. ELISA with different dilutions of soluble anti-HBs antibody A5 scFv. Periplasmic extract of untransformed HB2151^{Nal} cells were used as a negative control for the experiment and its binding to the antigen was considered as base line reading for the experiment.

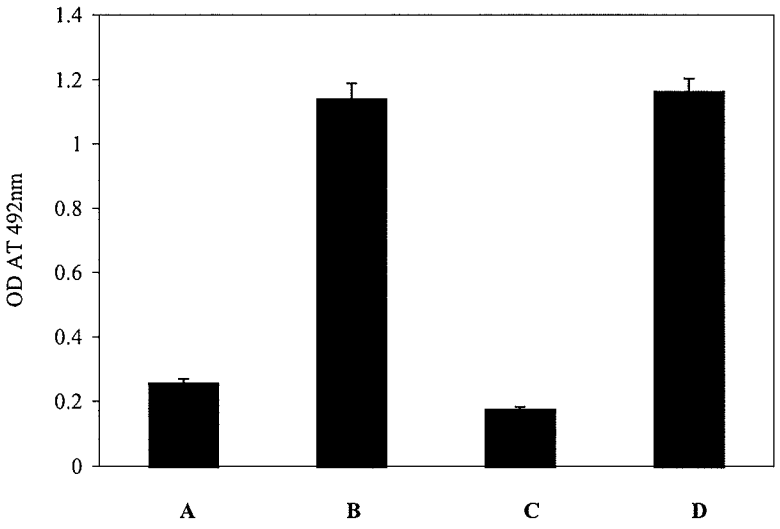

Fig. 3. Sandwich ELISA using 5S supernatant and A5 scFv. Antigen was captured in 5S hybridoma supernatant-coated ELISA plate and bound antigen was detected by sandwich ELISA. Bound antigen was detected by A5 scFv (B) and 5S hybridoma supernatant (D), both used at their saturating dilutions. In (A) scFv was added without any captured antigen, where as in (C) equivalent amount of untransformed HB2151^{Nal} extract was used to bind to the captured antigen.

involved in the complex formation, ELISAs were performed in presence of NaCl, urea and DMSO. NaCl is known to disturb the electrostatic interactions involved in protein–protein interactions and DMSO disturbs the hydrophobic forces. DMSO at high concentration is also a denaturing agent. As shown in the Fig. 4a, urea, a known destabilizing agent for antigen–antibody complexes had no significant effect on the binding of the scFv even at a concentration of 8 M. For the original mouse monoclonal 5S there was a decrease in binding as the concentration approached 8 M urea, but the

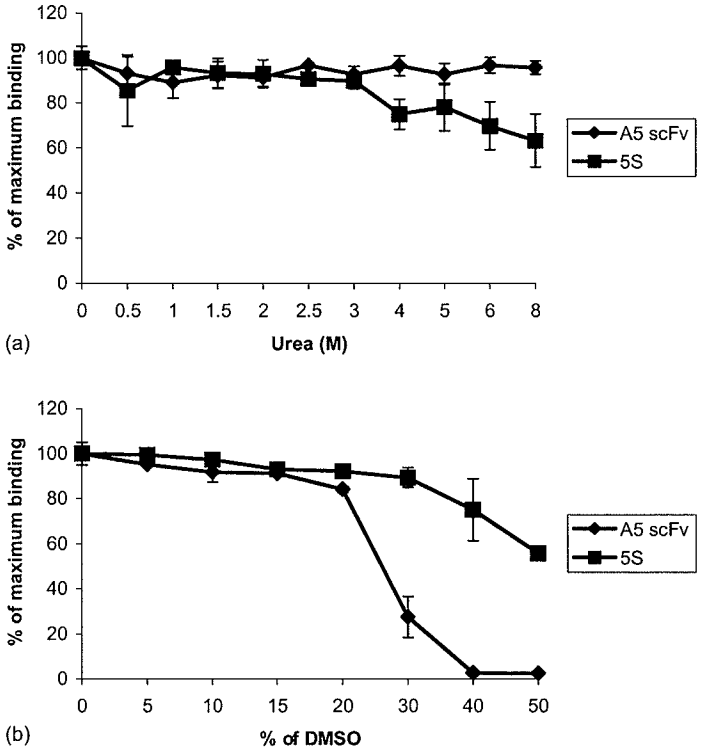

Fig. 4. Effects of urea and DMSO on antigen binding. (a) ELISA was done in presence of different concentration of urea, (b) similar experiment was performed in presence of DMSO.

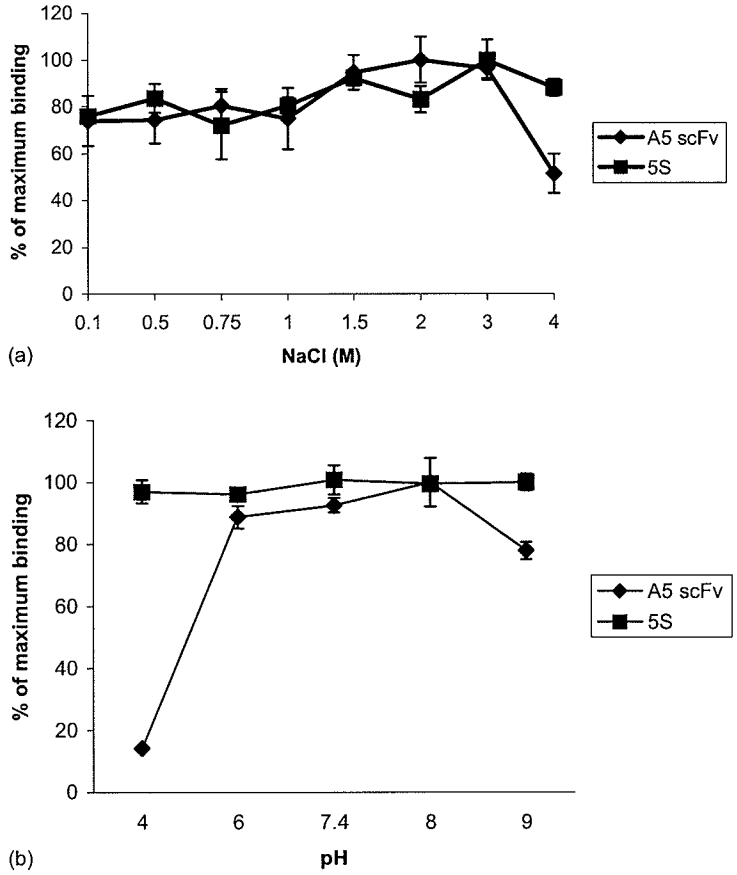

Fig. 5. ELISAs to investigate the effect of different concentrations of NaCl (a) and different pH (b) on antigen binding.

decrease was not very much, indicating that both the recombinant antibody and the 5S mouse monoclonal bind in a stable manner. Binding of 5S mouse monoclonal decreased only slightly with increase in DMSO concentration up to 50% indicating a high stability of the antigen–antibody complex (Fig. 4b). For the recombinant scFv A5, the binding was stable at 20% DMSO, but fell at 30%, indicating that some critical hydrophobic interaction between the antigen and the scFv could be disturbed by DMSO. Fig. 5a shows the binding profile of the recombinant antibody and the mouse monoclonal at different concentrations of NaCl. The mouse monoclonal shows stable binding even in presence of 4 M NaCl. However, there is a significant reduction in binding of A5 scFv at 4 M NaCl, perhaps due to disruption of electrostatic interactions. Involvement of electrostatic interactions is more evident when ELISA is performed at different pH. As shown in Fig. 5b, binding of the recombinant scFv remains unaltered in the pH range of 6–8 with a sharp fall in binding towards the lower side of the pH scale. However, the binding of the 5S mouse monoclonal remains unaltered over a much wider scale of pH. Fig. 6 shows the binding of the mouse monoclonal and the recombinant scFv fragment in presence of different concentrations of guanidium HCl. The mouse monoclonal 5S retained its binding to the antigen even at 2 M guanidium HCl. However, the binding of the recombinant scFv A5 decreased steadily with increasing concentration of guanidium HCl, indicating that the binding of the scFv is less stable than 5S.

3.7. Dissociation constant of the mouse monoclonal and its recombinant scFv

Dissociation constant, K_D, for both the scFv and whole antibody were determined by the method of Friguet et al. (1985). To meet the basic assumptions of the method, antigen was taken in excess to the antibody and all experiments were performed within the range of dilutions of the antibody, where absorbance in the ELISA changes linearly with dilution. As the interaction between coated antigen with the free/bound antibody can shift the equilibrium, we had incubated the overnight equilibrated antigen–antibody mixture, in antigen coated plate only for 20 min. This time is sufficient enough to measure the free antibody without causing considerable shift in the equilibrium (data not shown). As calculated from the slope of the straight lines in Fig. 7, the K_D values for scFv A5 and the whole antibody in 5S hybridoma supernatant are 0.9104 ± 0.5 nM ($R^2 = 0.9815$) and 0.8899 ± 0.3 nM ($R^2 = 0.9924$), respectively.

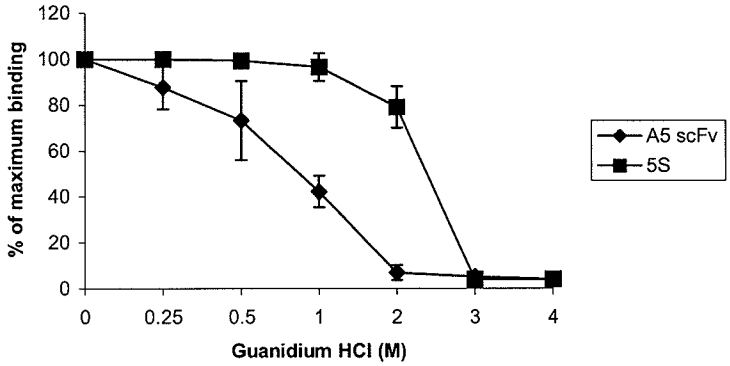

Fig. 6. Antigen binding by A5 scFv and 5S mouse monoclonal in the presence of different concentrations of guanidium hydrochloride as studied by ELISA.

3.8. Sequence analysis of variable region genes

Tables 1 and 2 show the sequence of the variable region of light and heavy chains. Amino acids are numbered as per the Kabat numbering scheme (Kabat et al., 1991). CDR regions are marked as per the Kabat definition except for CDR H1, which is defined as per Chothia and Lesk (1987) to include residues, that may be structurally important for antigen binding. Analysis of the amino acid sequences reveals that CDR L2, CDR L3 and CDR H1 are of type 1 canonical classes. CDR L1 belongs to class 4, CDR H2 is of class 2 and the 13 residue long CDR H3 has a kinked profile.

Homology search using V-Quest at IMGT, identifies that the light chain variable region of A5 scFv is of V_K1 class and has 90% (at amino acid level) identity with the germline light chain gene *IGKV1-117*02* (IMGT accession no. M28134). As shown in Table 1, the light chain variable region gene may have originated from the recombination of *IGKV1-117*02* and the J_K1 gene *IGKJ1*01* (IMGT accession no. V00777). The mutation at L2 may have originated due to the primer used during cloning. Out of the 14 other nucleotides changed from germline genes, 10 cause replacement mutations (six of which are clustered in CDRs). The ratios of replacement (R) to silent (S) mutation for light chain are 4/1 and 6/3 for FR and CDRs respectively. If replacement mutations take place randomly by chance, expected numbers of replacement mutations at FRs and at CDRs would be 7.5 and 3, respectively (Bagley et al., 1994; Ikematsu et al., 1994). Chi-square analysis shows that the number of replacement mutations at FR regions is significantly lower whereas at CDR regions, it is significantly higher than what would occur by random mutation by chance ($P = 0.031$).

The heavy chain variable region was found to be of highest homology with germline V_H gene *IGHV1S121*01* (IMGT accession no.: AF025445). It has 84.5% identity with this germline sequence in terms of amino acids. But the sequence of this gene is incomplete and is missing its C-terminal portion after the residue 82a. We searched the GenBank at NCBI and found that clone J558.42 has 100% similar sequence to that of IGH1S121 (GI: 11612052) and is complete one. Therefore, we used the sequence of J558.42, which has 86.7% homology with the mature antibody, for

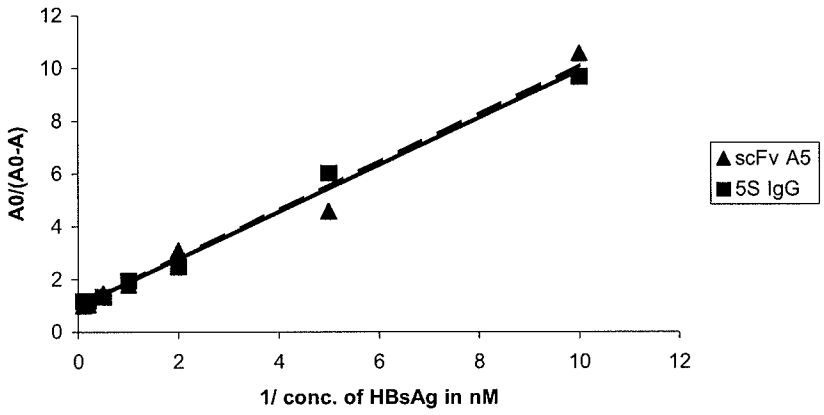

Fig. 7. Determination of average K_D of HBsAg-A5 scFv and HBsAg-5S IgG complexes. Dilutions of the scFv and whole antibody used for this experiments were 0.003 and 0.00075, respectively. Data points were fitted to the equation $A_0/(A_0 - A) = K_D/[Ag] + 1$, where A_0 is the absorbance when the antibody was incubated without any antigen, A absorbance corresponding to free antibody after incubation with antigen and [Ag] is the free antigen concentration which is equal to the antigen taken for experiment considering a pseudo-first-order reaction.

Table 1
Homology of the A5 scFv light chain with mouse germline genes

	2	3	4	5	6	7	8	9	10	11	12	13	14	15	16	17	18	19	20	21	22	23
VL A5 scFv	I	V	M	T	Q	T	P	L	S	L	P	V	S	L	G	D	Q	A	S	I	S	C
	ATT	GTG	ATG	ACC	CAG	ACT	CCA	CTC	TCC	CTG	CCT	GTC	AGT	CTT	GGA	GAT	CAA	GCC	TCC	ATC	TCT	TGC
IGKV1-117*02	G	---	---	---	---	--A	---	---	---	---	---	---	---	---	---	---	---	---	---	---	---	---
	V	*	*	*	*	*	*	*	*	*	*	*	*	*	*	*	*	*	*	*	*	*

	<----------CDR L1 ---------->																						
	24	25	26	27	27a	27b	27c	27d	27e	28	29	30	31	32	33	34	35	36	37	38	39		
VL A5 scFv	R	A	S	Q	S	I	V	H	S	Y	G	D	T	Y	L	E	W	H	L	Q	K		
	AGA	GCT	AGT	CAG	AGC	ATT	GTC	CAC	AGT	TAT	GGA	GAC	ACC	TAT	TTG	GAA	TGG	CAC	CTG	CAG	AAA		
IGKV1-117*02	---	T--	---	---	---	---	---	--A	--T	---	A--	---	A--	---	---	--A	---	---	T--	---	---	---	
	*	S	*	*	*	*	*	*	*	N	*	N	*	*	*	*	*	*	Y	*	*	*	

	<----------CDR L2 ---------->																						
	40	41	42	43	44	45	46	47	48	49	50	51	52	53	54	55	56	57	58	59	60	61	
VL A5 scFv	P	G	Q	S	P	K	L	L	I	Y	K	V	S	N	R	F	S	G	V	P	D	R	
	CCA	GGC	CAG	TCT	CCA	AAG	CTC	CTG	ATC	TAC	AAA	GTT	TCC	AAC	CGA	TTT	TCT	GGG	GTC	CCA	GAC	AGG	
IGKV1-117*02	---	---	---	---	---	---	---	---	---	---	---	---	---	---	---	--	G---	---	---	---	---	---	
	*	*	*	*	*	*	*	*	*	*	*	*	*	*	*	L	*	*	*	*	*	*	

	62	63	64	65	66	67	68	69	70	71	72	73	74	75	76	77	78	79	80	81	82		
VL A5 scFv	F	S	G	S	G	S	G	T	E	F	T	L	K	I	S	R	V	E	A	E	D		
	TTC	AGT	GGC	AGT	GGA	TCA	GGG	ACA	GAA	TTC	ACA	CTC	AAG	ATC	AGC	AGA	GTG	GAG	GCT	GAG	GAT		
IGKV1-117*02	---	---	---	---	---	---	---	---	--Y	---	---	---	---	---	---	---	---	---	---	---	---		
	*	*	*	*	*	*	*	*	D	*	*	*	*	*	*	*	*	*	*	*	*		

	<---------- CDR L 3 ---------->																						
	83	84	85	86	87	88	89	90	91	92	93	94	95	96	97	98	99	100	101	102	103		
VL A5 scFv	L	G	V	Y	F	C	F	Q	R	S	Y	V	P	W	T	F	G	G	G	T	K		
	CTG	GGA	GTT	TAT	TTC	TGC	TTT	CAA	CGT	TCA	TAT	GTT	CCG	TGG	ACG	T TC	GGT	GGA	GGC	ACC	AAG		
IGKV1-117*02	---	---	---	---	-A-	---	---	---	G--	---	C--	---	---	T CC									
	*	*	*	*	Y	*	*	*	G	*	H	*	*										
IGKJ1*01													-	---	---	---	---	---	---	---	---		
														*	*	*	*	*	*	*	*		

	104	105	106	107	108	
VL A5 scFv	L	E	L	K	R	
	CTG	GAA	CTC	AAA	CGG	
IGKJ1*01	---	---	A--	---	---	
	*	*	I	*	*	

Nucleotide and amino acid sequence of A5 scFv light chain variable region aligned with most homologous germline V region (*IGKV1-117*02*, IMGT code: M28134) and J region (*IGKJ1*01*, IMGT code: V00777) genes. In case of germline genes, only the differences in nucleotide and amino acids are shown. Amino acids are numbered according to the Kabat numbering scheme. EMBL accession number for the sequence of A5 scFv is AJ549501.

further analysis. As shown in Table 2, C-terminal region of the antibody may have originated from the recombination of germline genes *IGHD-SP2.5*01*, *IGHJ4*01* (IMGT accession no: J00432, V00770, respectively) with probable insertion of seven bases at the 5-end of the D gene. Apart from the mutation at the first residue, which may have originated due to the cloning primer, 22 other mutations have generated 15 replacement mutations. The ratios for replacement to silent mutation are 8/2 (expected $R = 5.6$) and 7/5 (expected $R = 11.5$) for CDR regions and FR regions, respectively. Although in CDR regions there is a bias towards replacement mutations over silent ones, no significant bias can be identified for replacement mutations in CDR regions over FRs (P value for chi-square test is 0.095).

3.9. Structural significance of somatic mutations

In order to study the importance of the hypermutated residues, we modeled the variable regions of the antibody and its germline counterpart, using WAM, web based antibody modeler (Whitelegg and Rees, 2000). Additionally, we have used the information on the importance of a particular residue as observed in antibodies with known structure from the data available at " AHo's Amazing Atlas of Antibody Anatomy, AAAAA" (http://www.unizh.ch/~antibody) (Honegger and Pluckthun, 2001). The quality of both the WAM modeled antibody structures, was determined by examining the distribution of amino acids residues in the Ramachandran plot (Ramachandran and Sasisekharan, 1968).

Table 2
Homology of the A5 scFv heavy chain with mouse germline genes

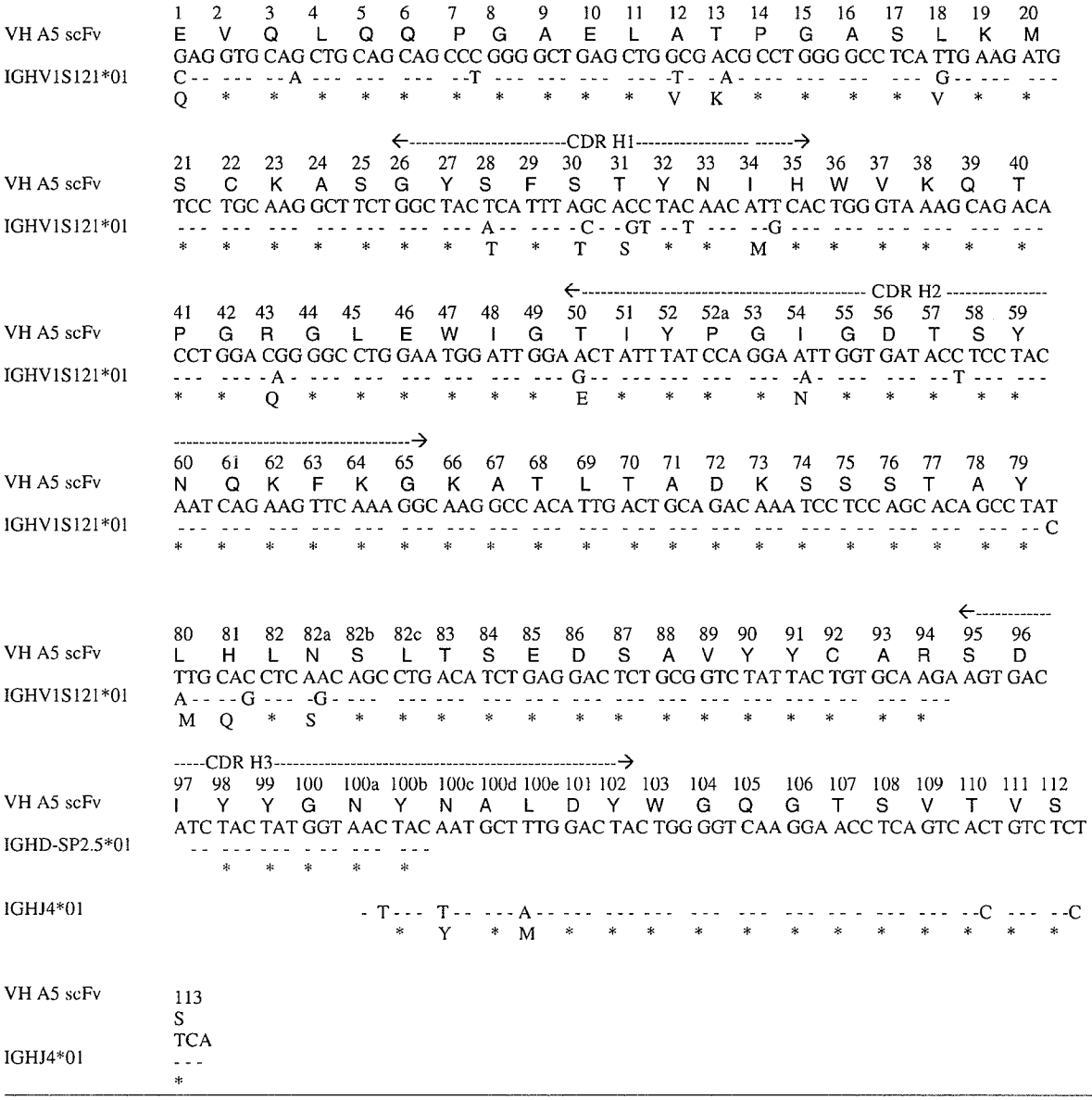

Nucleotide and amino acid sequence of A5 scFv heavy chain variable region aligned with most homologous germline V region (*IGHV1S121*01*), D region (*IGHD-SP2.5*01*) and J region (*IGHJ4*01*) genes. In case of germline genes, only the differences in nucleotide and amino acids are shown. Amino acids are numbered according to Kabat numbering scheme. EMBL accession number for the sequence of A5 scFv is AJ549501.

In both the structures only about 7% residues are present in disallowed regions and majority of those residues are glycine.

The WAM models show that for both the mature and germline antibody, the paratope is a deep groove with more negative charge in case of the germline one. Canonical classes for CDRs are same, both in the germline as well as mature antibody. There is no significant difference in the overall backbone conformation of the mature antibody and its germline counterpart, as the rms shift is only 0.23 Å. Significant deviations in backbone are observed only in CDR L1 and in CDR H3 (Fig. 8a).

3.9.1. Mutations at the binding site

Positions of replacement mutations originated by somatic mutations, as predicted by molecular modeling are shown in Table 3. The hypermutation at H50 from Glu to Thr destroys the negative charge at that region as well as makes the cavity deeper. Another mutation at the base of the binding face is His L93 to Tyr L93. Tyr L93 is usually very rare in this

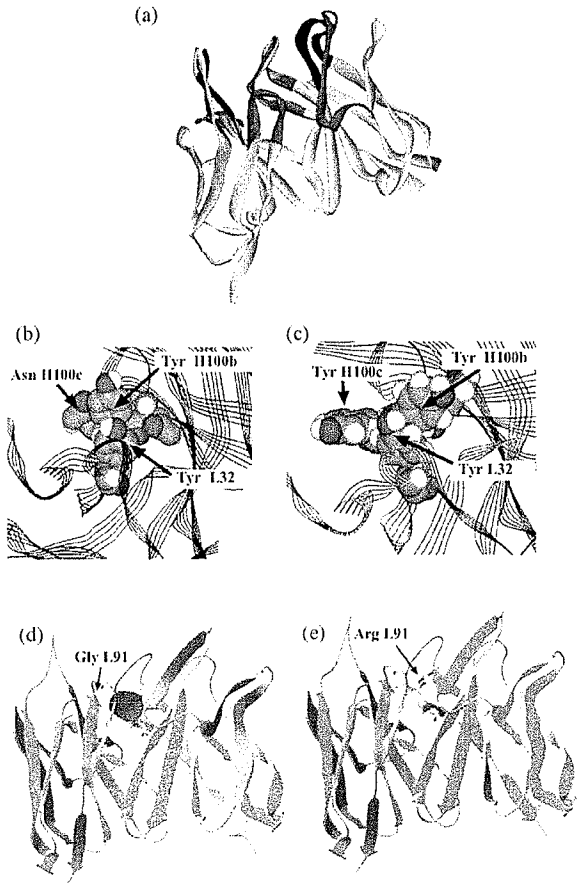

Fig. 8. (a) Ribbon diagram of A5 scFv variable regions is superimposed with that of its germline counterpart. CDR1, 2 and 3 for both the chains are coloured as blue, green and red, respectively. CDR H3 for the mature antibody shows significant movement from that of the germline one. The CDR H3 for germline antibody that shows deviation is yellow in colour. Similar movement is observed in case of CDR L1 of mature antibody (germline CDR L1 is yellow in colour). Somatic mutations at the V_L/V_H interface help in better packing of residues at the interface. (b) The packing of Tyr H100b and Tyr L32 in mature antibody, (c) the packing of Tyr H100b and Tyr L32 in the germline. Mutation at H100c replaces Tyr with Asn, giving Tyr H100b more space and better aromatic stacking. In the ribbon diagram (d) the solvent inaccessible cavity is shown in red at the interface of heavy and light chains in the germline antibody. Somatic mutation at L91 Gly → Arg allows better inter-chain packing in the mature antibody (e). The molecular models were obtained through modeling using WAM. Diagrams were generated using Accelrys ViewerLite Version 5.0 and SwissPdb Viewer. (For interpretation of the references to color in this figure legend, the reader is referred to the web version of this article.)

Table 3
Somatic replacement mutations in A5 scFv

Light chain		
Binding site		
Asn L28 → Tyr	CDR1	
Asn L30 → Asp	CDR1	
His L93 → Tyr	CDR3	
V_H/V_L interface		
Tyr L36 → His	FR2	TAC motif
Leu L55 → Phe	CDR2	
Gly L91 → Arg	CDR3	
Solvent exposed, away from binding site		
Asp L70 → Glu	FR3	
Tyr L87 → Phe	FR3	
Ile L106 → Leu	FR4	
Solvent inaccesible, away from binding site		
Ser L25 → Ala	CDR1	
Heavy chain		
Binding site		
Glu H50 → Thr	CDR2	RGYW motif
Asn H54 → Ile	CDR2	
V_H/V_L interface:		
Tyr H100c → Asn	CDR3	
Met H100e → Leu	CDR3	
Solvent exposed, away from binding site		
Val H12 → Ala	FR1	
Lys H13 → Thr	FR1	AANB motif
Thr H28 → Ser	CDR1	
Thr H30 → Ser	CDR1	WDCH motif
Ser H31 → Thr	CDR1	RGYW motif
Gln H43 → Arg	FR2	
Gln H81 → His	FR3	DGHD motif
Ser H82a → Asn	FR3	RGYW motif
Solvent inaccesible, away from binding site		
Val H18 → Leu	FR1	DGHD motif
Met H34 → Ile	CDR1	DGHD motif
Met H80 → Leu	FR3	

List of somatic replacement mutations present in 5S are listed as per their structural positions. Known hypermutation motifs (Smith et al., 1996 and Dunn-Walters et al., 1998) are shown in the extreme right column.

position (in 2% of protein antigens and in 2% of oligomeric antigens) and forms an extended palm like structure. It is well established that antigen binding sites are usually rich in tyrosine and such residues are usually involved in antigen binding (Padlan, 1990). In total, the antigen binding face of this antibody has six tyrosine residues of which two have originated by mutation from the germline.

Residues of CDR L1 form a projected finger like structure. This loop has three mutations making the fingertip tilt more towards the center of the cavity as compared to the germline structure, with Ser L27e showing maximum rms deviation of 1.323 Å. CDR H3 has two mutations. Though CDR H3 of both germline and mature antibody show similar kinked backbone structures, they show significant rms deviation with the mutated mature loop moving away from the deep groove (Fig. 8a). In our study the CDR H3 has a kinked base with a β-loop that does not show a hydrogen bond ladder and belongs to class B (Shirai et al., 1999). Shirai et al. (1999) had shown that a CDR H3 having such a β-loop structure is less flexible and shows very little movement upon antigen binding (rms < 0.8 Å).

3.9.2. Mutations at heavy and light chains interface

Apart from critical mutations at the binding site there are five replacement mutations at the V_H/V_L interface. Y L32, present at the base of the projecting CDR L1 is at the

interface of heavy and light chains and faces Asn H100a, Tyr H 100b, Asn H100c. In the germline sequence, H100c is tyrosine. Comparison of molecular models indicates that such a mutation is important for better accommodation of interface residues and better stacking of Tyr H100b with Tyr L32 (Fig. 8b and c).

The region of CDR H3, which bears two mutations, is at the heavy and light chains interface. This region interacts with eight amino acids of light chain, three of which have mutated from their germline residue. As shown in the Fig. 8d, there is a solvent inaccessible cavity in between V_H and V_L in the germline structure, which is not present in case of the mature antibody due to the presence of Arg L91 (Fig. 8e), indicating better packing of V_H and V_L.

3.9.3. Mutations away from the binding site

In case of the light chain, two other mutated residues Asp L70 and Leu L106 are present on the surface, away from the binding site where mutations are well tolerated. The heavy chain has eight such mutations, which are solvent exposed, away from binding site and can be well tolerated by the antibody structure. Ala L25, Leu H18, Ile H34, Leu H80 are away from binding site and are not solvent exposed. Data base analysis of antibodies of known structure shows that these amino acids are very frequent in their respective positions, again confirming that these must be well tolerated.

4. Discussion

Passive immunization by anti-HBs antibody is usually indicated in cases of post-exposure prophylaxis. Till date different forms of recombinant antibodies have been reported against immunogenic determinants of HBV, though none of them are clinically available (Li et al., 1990; Park et al., 2000; Maeda et al., 1999). We have cloned and expressed a mouse monoclonal (5S) against HBsAg that retains antigen binding in the presence of agents that usually destabilize protein–protein interactions. The use of a stringent screening method, for both the screening of immunized animals and also for hybridoma supernatants, was instrumental in obtaining a hybridoma with very stable and high affinity binding. This hybridoma retains its binding to the antigen in the presence of 8 M urea, 30% DMSO, 4 M NaCl and at extremes of pH. It has an affinity of 0.8899 nM. This monoclonal also tested positive in an in vitro assay that is a surrogate indicator for sero-conversion and for protective antibodies. The recombinant antibody fragment A5 scFv binds to the antigen with very high affinity and has an apparent dissociation constant equivalent to that of the original mouse monoclonal. Such an observation is quite unusual because, antibody fragments like scFv usually show different kinetics from that of the full-length immunoglobulin due to steric factors. Competition experiments have shown that the recombinant scFv binds to the same epitope as the mouse monoclonal.

The scFv also retains antigen binding in the presence of 8 M urea, 20% DMSO and 3 M NaCl. The extent of tolerance to DMSO is an indicator of the strength of hydrophobic interactions involved in conformational stability and in stabilizing protein–protein interaction. While the parent monoclonal retained 80% binding even at 40% DMSO, there was a sharp drop in binding of the scFv above 20%. Urea is known to destabilize antigen–antibody interactions by breaking hydrogen bonds. The anomalous behavior in the presence of increased concentration of urea is interesting, as the binding for the parent monoclonal, 5S, decreased at concentrations more than 3 M urea. However, the binding of the scFv A5 is not altered even at 8 M urea. Electrostatic interactions involved in protein–protein interaction are disturbed by high concentrations of salt and at high/low pH. While in absolute terms, the binding of A5 tolerates a fairly high concentration of NaCl (3 M), it is less than that of 5S (which retains binding at 4 M NaCl). The pH range for scFv binding is also less than that of the mouse monoclonal. A5 retains 80% of its binding between pH 6–9, while 5S retains binding over a much broader range. Reduction in the binding of A5 scFv in presence of 4 M NaCl and at extremes of pH indicates the involvement of electrostatic interactions in antigen–antibody complex formation, which are not present, or not of significance in case of the full-length antibody 5S. scFvs are known to have different physical properties at different pH ranges, which affects their binding. Kuttner et al. (1999) have reported about an anti-pre S1 scFv, which retains its binding even at pH 11 and loses binding only at pH 1.5. Pedroso et al. (2002) have shown that an anti-HBs scFv retains its native, monomeric form only in the pH range of 7–11 and forms aggregates below pH 6. Our experiments show that, while both the mouse monoclonal and the recombinant scFv binds to the antigen with comparably high affinity and stability, there are differences in the nature of molecular forces that determine the stability of either the individual components or of the antigen–antibody complex. Stable binding of the mouse monoclonal 5S is also evident from the fact that it retains binding even in the presence of 1 M guanidium HCl. Binding of its scFv fragment decreases steadily with increasing concentration of guanidium HCl. It is known that antibody variable domains have evolved to fold and dimerize in order to generate the binding site, whereas the dimerization of constant domains provides stability for the whole structure. Absence of constant domains in the scFv may explain the comparatively lower tolerance of its antigen binding to agents that destabilize protein structure.

Sequence analysis of the antibody heavy and light chains indicates that it belongs to the canonical class of 1-2-4-1-1 (i.e. H1-H2-L1-L2-L3). Usually antibodies binding to protein antigens have a large flat paratope, whereas those binding to small molecules show deep grooves. Sequence analysis of antibodies in Kabat database indicates that the canonical structural class of 1-2-4-1-1 (i.e. H1-H2-L1-L2-L3) is predominantly present in cases of antibodies binding to peptide antigens, as it provides deep

groove for antigen binding (Vargas-Madrazo et al., 1995). We also searched the protein database for antibodies with similar canonical structure and loop lengths and found that majority of them bind to small antigens. Although not very common, a few of the antibodies against pathogenic antigens have similar canonical structures and loop lengths as of 5S; thus having a deep binding pocket for specific and tight binding (Wien et al., 1995; Fleury et al., 1999; Lescar et al., 1999; van Den Elsen et al., 1997). Two anti-pre S1 antibodies also have deep groove like binding sites (Pizarro et al., 2001; Kuttner et al., 1999).

We have also analyzed the mutations, which were generated during affinity maturation of the antibody through somatic hypermutations. In case of the light chain of 5S, the number of replacement mutations in the CDR regions is significantly higher than that would occur by random mutations by chance, whereas it is significantly lower in FR regions. Such a biased distribution of replacement mutations is usually considered as the feature of antigen driven clonal selection (Ikematsu et al., 1994). However, no such skewed distribution of replacement mutation was observed in case of the heavy chain of the antibody. Analysis of codon usage in immunogloubulin genes strongly suggests that these sequences have evolved to ensure proper localization of somatic hypermutations so that the specific antibody can evolve without searching infinite shape space (Wagner et al., 1995). In fact immunogloublin genes have intrinsic mutational hot spots like RGYW motif (Smith et al., 1996) and the intrinsic hypermutability decreases exponentially towards 3′-end (Rada and Milstein, 2001). Mutations at position H31, H50 and H82a of this anti-HBs antibody have the RGYW motif and are established hot spots for somatic hypermutation. In the light chain, the codon TAC at L36 is another mutational hotspot (Smith et al., 1996). While analyzing a mature antibody sequence it should be kept in mind that it is the resultant of intrinsically biased hypermutation and of antigenic selection for specific and enhanced binding. Therefore, the difference in the results for the heavy and light chains of A5 scFv, indicates that statistical analysis can be only one of the indicators for stating reliably that antigenic selection of the B cell carrying the antibody gene has occurred (Dunn-Walters and Spencer, 1998).

Till date the crystal structure of HBsAg has not been elucidated, limiting the understanding of structural aspects of anti-HBs antibodies. Nair et al. (2000) have determined the crystal structure of an anti-HBs antibody in complex with the peptide corresponding to one B cell epitope of the antigen. Since antibodies have highly conserved structures and are one of the best-studied families of proteins using X-ray crystallography, molecular modeling of an antibody molecule can generate reliable information. Molecular modeling and analysis of variable regions of 5S and its germline counterpart indicates that several critical mutations are present in the V_H/V_L interface and at the binding site. The mutation at H50 from Glu to Thr reduces the overall negative charge in the deep binding pocket. It is worthnoting that position H50 is a mutational hotspot and the observed mutation at this position may be essential for binding of the antigen. Another important observation is the deviation of CDR H3 and CDR L1 from their germline positions. As the β-loop of CDR H3 of 5S is not very flexible; movement of CDR H3 from its germline position may be essential for better fitting of the antigen in the binding pocket. Similar movements have been observed in the cases of hapten binding antibodies, where somatic mutations caused movement of CDR H3 to stabilize the "lock and key" arrangement (Yin et al., 2001; Wedemayer et al., 1997). It was further observed that mutations at the V_H/V_L interface provide better inter-chain packing. One of the important mutations at the V_H/V_L interface is from Asn to Tyr at H100c. The comparison of molecular modeling results indicates that such a mutation is important for a better accommodation of interface residues and better stacking of Tyr H100b with Tyr L32. The mature antibody also shows superior inter-chain packing. There is a solvent inaccessible cavity at the V_H/V_L interface of the model of the germline molecule. The mutation at L91 from Gly to Arg in the mature antibody helps in the improvement of inter-chain packing by removing this cavity.

There are 15 other mutations generated during affinity maturation, which are away from binding site and whose structural importance is difficult to understand. Ramierez-Benitez and Almagro (2001) have shown that majority of the amino acids replaced by somatic hypermutations are usually not in contact with antigen. Such distant residues also contribute to affinity and specificity of an antibody (Daugherty et al., 2000; Kala et al., 2002). Cumbers et al. (2002) had shown that, at the initial phase of affinity maturation low affinity binders are generated through mutations at critical residues at CDRs but further maturation takes place by strategic framework mutations. Gonzalez-Fernandez and Milstein (1998) have shown that low-dose immunization favors the selection of a more focused mutational pattern, with a low mutational background. Such background mutations are either conservative mutations, or present on the outer surface away from the binding site and well tolerated.

Although high affinity and stability do not always assure in vivo viral neutralization, these are certainly the basic requirement for a neutralizing antibody. As neutralization is directly correlated to the occupancy of sites on the virion and inhibition of virus attachment (Burton et al., 2000; Klasse and Sattentau, 2002), high affinity and stability of binding under different conditions in the physiological microenvironment are essential for a neutralizing antibody. It has been shown that high affinity and in vitro stability of recombinant antibody fragments have direct correlation with their in vivo function (Maynard et al., 2002; Willuda et al., 1999). Therefore, the mouse monoclonal 5S which has very high affinity and forms a stable antigen–antibody complex can be a potent therapeutic molecule. However, it can be used clinically only after humanization through recombinant approach to prevent any possible HAMA response.

Recombinant antibody fragments like scFv have the advantage that they can be easily expressed in a bacterial system and can be modified and screened for humanization. The recombinant scFv of this antibody shows similar binding and kinetic properties as of the whole antibody. Further manipulation of this recombinant scFv can lead us towards a recombinant mouse–human chimeric or humanized antibody, which can be safely utilized for passive immunization in case of HBV infection. In addition to the generation of potentially therapeutic antibodies, this study could help in our understanding of the evolution of stable, high affinity interaction during the maturation of the antibody response.

Acknowledgements

This work has been funded from research grants from the Department of Biotechnology, India and Indian Council of Medical Research, India. We thank Prof. Greg Winter for kindly gifting us the vector pHEN1, and Dr Vijay Chaudhary for his gift of anti-M13 monoclonal antibody. We also thank Ashutosh Tiwari for helpful discussion and help during isolation of clones. We are thankful to M/s Mathura Prasad and Satish for their technical and secretarial assistance.

References

Altschul, S.F., Gish, W., Miller, W., Myers, E.W., Lipman, D.J., 1990. Basic local alignment search tool. J. Mol. Biol. 215, 403–410.

Bagley, J., Dillon, P.J., Rosen, C., Robinson, J., Sodroski, J., Marasco, W.A., 1994. Structural characterization of broadly neutralizing human monoclonal antibodies against the CD4 binding site of HIV-1 gp120. Mol. Immunol. 31, 1149–1160.

Barbas III, C.F., Burton, D.R., Scott, J.K., Silverman, G.J., 2001. Phage Display: A Laboratory Manual, first ed. Cold Spring Harbor Laboratory Press, Cold Spring Harbor, NY.

Bernstein, F.C., Koetzle, T.F., Williams, G.J., Meyer Jr., E.F., Brice, M.D., Rodgers, J.R., Kennard, O., Shimanouchi, T., Tasumi, M., 1977. The Protein Data Bank: a computer-based archival file for macromolecular structures. J. Mol. Biol. 112, 535–542.

Burton, D.R., Williamson, R.A., Parren, P.W., 2000. Antibody and virus: binding and neutralization. Virology 270, 1–3.

Chothia, C., Lesk, A.M., 1987. Canonical structures for the hypervariable loops of immunoglobulins. J. Mol. Biol. 196, 901–917.

Cumbers, S.J., Williams, G.T., Davies, S.L., Grenfell, R.L., Takeda, S., Batista, F.D., Sale, J.E., Neuberger, M.S., 2002. Generation and iterative affinity maturation of antibodies in vitro using hypermutating B-cell lines. Nat. Biotechnol. 20, 1129–1134.

Dauber-Osguthorpe, P., Roberts, V.A., Osguthorpe, D.J., Wolff, J., Genest, M., Hagler, A.T., 1988. Structure and energetics of ligand-binding to proteins: *Escherichia coli* dihydrofolate reductase/trimethoprim, a drug-receptor system. Proteins 4, 31–47.

Daugherty, P.S., Chen, G., Iverson, B.L., Georgiou, G., 2000. Quantitative analysis of the effect of the mutation frequency on the affinity maturation of single chain Fv antibodies. Proc. Natl. Acad. Sci. U.S.A. 97, 2029–2034.

De Maeyer, M., Desmet, J., Lasters, I., 2000. The dead-end elimination theorem: mathematical aspects, implementation, optimizations, evaluation, and performance. Methods Mol. Biol. 143, 265–304.

Dunn-Walters, D.K., Spencer, J., 1998. Strong intrinsic biases towards mutation and conservation of bases in human IgVH genes during somatic hypermutation prevent statistical analysis of antigen selection. Immunology 95, 339–345.

Dunn-Walters, D.K., Dogan, A., Boursier, L., MacDonald, C.M., Spencer, J., 1998. Base-specific sequences that bias somatic hypermutation deduced by analysis of out-of-frame human IgVH genes. J. Immunol. 160, 2360–2364.

Fleury, D., Barrere, B., Bizebard, T., Daniels, R.S., Skehel, J.J., Knossow, M., 1999. A complex of influenza hemagglutinin with a neutralizing antibody that binds outside the virus receptor binding site. Nat. Struct. Biol. 6, 530–534.

Friguet, B., Chaffotte, A.F., Djavadi-Ohaniance, L., Goldberg, M.E., 1985. Measurements of the true affinity constant in solution of antigen–antibody complexes by enzyme-linked immunosorbent assay. J. Immunol. Methods 77, 305–319.

Gamelkoorn, G.J., 1991. Case study: Hepatitis B vaccine: a product of r-DNA techniques. In: Turnock, G. (Ed), Biotechnological Innovations in Health Care. Butterworth Heinemann, Guildford, UK, pp. 141–164.

Gonzalez-Fernandez, A., Milstein, C., 1998. Low antigen dose favours selection of somatic mutants with hallmarks of antibody affinity maturation. Immunology 93, 149–153.

Guex, N., Peitsch, M.C., 1997. SWISS-MODEL and the Swiss-PdbViewer: an environment for comparative protein modeling. Electrophoresis 18, 2714–2723.

Harlow, E., Lane, D., 1988. Antibodies: A Laboratory Manual. Cold Spring Harbor Laboratory Press, Cold Spring Harbor, NY.

Honegger, A., Pluckthun, A., 2001. Yet another numbering scheme for immunoglobulin variable domains: an automatic modeling and analysis tool. J. Mol. Biol. 309, 657–670.

Hoogenboom, H.R., Winter, G., 1992. By-passing immunisation: human antibodies from synthetic repertoires of germline VH gene segments rearranged in vitro. J. Mol. Biol. 227, 381–388.

Ikematsu, H., Ichiyoshi, Y., Schettino, E.W., Nakamura, M., Casali, P., 1994. VH and V kappa segment structure of anti-insulin IgG autoantibodies in patients with insulin-dependent diabetes mellitus: evidence for somatic selection. J. Immunol. 152, 1430–1441.

Kabat, E.A., Wu, T.T., Perry, H.M., Gottesman, K.S., Foeller, C., 1991. Sequences of Proteins of Immunological Interest, fifth ed. US Department of Health and Human Services, NIH, Bethesda, MD.

Kala, M., Bajaj, K., Sinha, S., 2001. Direct antigen capture by soluble scFv antibodies: a method for detection, characterization, and determination of affinity. Appl. Biochem. Biotechnol. 90, 11–22.

Kala, M., Misra, A., Saini, D., Bajaj, K., Sinha, S., 2002. Phage display antibodies to heat stable alkaline phosphatase: framework region as a determinant of specificity. J. Biochem. 132, 535–541.

Klasse, P.J., Sattentau, Q.J., 2002. Occupancy and mechanism in antibody-mediated neutralization of animal viruses. J. Gen. Virol. 83 (Pt 9), 2091–2108.

Kuttner, G., Kramer, A., Schmidtke, G., Giessmann, E., Dong, L., Roggenbuck, D., Scholz, C., Seifert, M., Stigler, R.D., Schneider-Mergener, J., Porstmann, T., Hohne, W., 1999. Characterization of neutralizing anti-pre-S1 and anti-pre-S2 (HBV) monoclonal antibodies and their fragments. Mol. Immunol. 36, 669–683.

Lefranc, M.P., 2001. IMGT, the international ImMunoGeneTics database. Nucleic Acids Res. 29, 207–209.

Lescar, J., Brynda, J., Rezacova, P., Stouracova, R., Riottot, M.M., Chitarra, V., Fabry, M., Horejsi, M., Sedlacek, J., Bentley, G.A., 1999. Inhibition of the HIV-1 and HIV-2 proteases by a monoclonal antibody. Protein Sci. 8, 2686–2696.

Li, Y.W., Lawrie, D.K., Thammana, P., Moore, G.P., Shearman, C.W., 1990. Construction, expression and characterization of a murine/human chimeric antibody with specificity for hepatitis B surface antigen. Mol. Immunol. 27, 303–311.

Maeda, F., Nagatsuka, Y., Ihara, S., Aotsuka, S., Ono, Y., Inoko, H., Takekoshi, M., 1999. Bacterial expression of a human recombinant monoclonal antibody fab fragment against hepatitis B surface antigen. J. Med. Virol. 58, 338–345.

Maynard, J.A., Maassen, C.B., Leppla, S.H., Brasky, K., Patterson, J.L., Iverson, B.L., Georgiou, G., 2002. Protection against anthrax toxin by recombinant antibody fragments correlates with antigen affinity. Nat. Biotechnol. 20, 597–601.

McAuliffe, V.J., Purcell, R.H., Gerin, J., 1980. Type B Hepatitis: a review of current prospects for a safe and effective vaccine. Rev. Infect. Dis. 2, 470–492.

Milich, D.R., Chen, M., Schodel, F., Peterson, D.L., Jones, J.E., Hughes, J.L., 1997. Role of B cells in antigen presentation of the Hepatitis B core. Proc. Natl. Acad. Sci. U.S.A. 94, 14648–14653.

Nair, D.T., Singh, K., Sahu, N., Rao, K.V., Salunke, D.M., 2000. Crystal structure of an antibody bound to an immunodominant peptide epitope: novel features in peptide-antibody recognition. J. Immunol. 165, 6949–6955.

Padlan, E.A., 1990. On the nature of antibody combining sites: unusual structural features that may confer on these sites an enhanced capacity for binding ligands. Proteins 7, 112–124.

Park, S.S., Ryu, C.J., Kang, Y.J., Kashmiri, S.V., Hong, H.J., 2000. Generation and characterization of a novel tetravalent bispecific antibody that binds to Hepatitis B virus surface antigens. Mol. Immunol. 37, 1123–1130.

Pedroso, I., Irun, M.P., Machicado, C., Sancho, J., 2002. Four-state equilibrium unfolding of an scFv antibody fragment. Biochemistry 41, 9873–9884.

Pizarro, J.C., Vulliez-le Normand, B., Riottot, M.M., Budkowska, A., Bentley, G.A., 2001. Structural and functional characterization of a monoclonal antibody specific for the preS1 region of Hepatitis B virus. FEBS Lett. 509, 463–468.

Rada, C., Milstein, C., 2001. The intrinsic hypermutability of antibody heavy and light chain genes decays exponentially. EMBO J. 20, 4570–4576.

Ramachandran, G.N., Sasisekharan, V., 1968. Conformation of polypeptides and proteins. Adv. Protein Chem. 23, 283–438.

Ramierez-Benitez, M.C., Almagro, J.C., 2001. Analysis of antibodies of known structure suggests a lack of correspondence between the residues in contact with the antigen and those modified by somatic hypermutation. Proteins 45, 199–206.

Sambrook, J., Russell, D., 2001. Molecular Cloning: A Laboratory Manual, third ed. Cold Spring Harbor Laboratory Press, Cold Spring Harbor, NY.

Shearer, M.H., Sureau, C., Dunbar, B., Kennedy, R.C., 1998. Structural characterization of viral neutralizing monoclonal antibodies to Hepatitis B surface antigen. Mol. Immunol. 35, 1149–1160.

Shirai, H., Kidera, A., Nakamura, H., 1999. H3-rules: identification of CDR-H3 structures in antibodies. FEBS Lett. 455, 188–197.

Smith, D.S., Creadon, G., Jena, P.K., Portanova, J.P., Kotzin, B.L., Wysocki, L.J., 1996. Di- and trinucleotide target preferences of somatic mutagenesis in normal and autoreactive B cells. J. Immunol. 156, 2642–2652.

Sureau, C., Moriarty, A.M., Thornton, G.B., Lanford, R.E., 1992. Production of infectious hepatitis delta virus in vitro and neutralization with antibodies directed against Hepatitis B virus pre-S antigens. J. Virol. 66, 1241–1245.

Tada, H., Yanagida, M., Mishina, J., Fujii, T., Baba, K., Ishikawa, S., Aihara, S., Tsuda, F., Miyakawa, Y., Mayumi, M., 1982. Combined passive and active immunization for preventing perinatal transmission of Hepatitis B virus carrier state. Pediatrics 70, 613–619.

van Den Elsen, J.M., Herron, J.N., Hoogerhout, P., Poolman, J.T., Boel, E., Logtenberg, T., Wilting, J., Crommelin, D.J., Kroon, J., Gros, P., 1997. Bactericidal antibody recognition of a PorA epitope of *Neisseria meningitidis*: crystal structure of a Fab fragment in complex with a fluorescein-conjugated peptide. Proteins 29, 113–125.

Vargas-Madrazo, E., Lara-Ochoa, F., Almagro, J.C., 1995. Canonical structure repertoire of the antigen-binding site of immunoglobulins suggests strong geometrical restrictions associated to the mechanism of immune recognition. J. Mol. Biol. 254, 497–504.

Wagner, S.D., Milstein, C., Neuberger, M.S., 1995. Codon bias targets mutation. Nature 376, 732.

Wedemayer, G.J., Patten, P.A., Wang, L.H., Schultz, P.G., Stevens, R.C., 1997. Structural insights into the evolution of an antibody combining site. Science 276, 1665–1669.

Whitelegg, N.R., Rees, A.R., 2000. WAM: an improved algorithm for modelling antibodies on the WEB. Protein Eng. 13, 819–824.

Wien, M.W., Filman, D.J., Stura, E.A., Guillot, S., Delpeyroux, F., Crainic, R., Hogle, J.M., 1995. Structure of the complex between the Fab fragment of a neutralizing antibody for type 1 poliovirus and its viral epitope. Nat. Struct. Biol. 2, 232–243.

Willuda, J., Honegger, A., Waibel, R., Schubiger, P.A., Stahel, R., Zangemeister-Wittke, U., Pluckthun, A., 1999. High thermal stability is essential for tumor targeting of antibody fragments: engineering of a humanized anti-epithelial glycoprotein-2 (epithelial cell adhesion molecule) single-chain Fv fragment. Cancer Res. 59, 5758–5767.

Yin, J., Mundorff, E.C., Yang, P.L., Wendt, K.U., Hanway, D., Stevens, R.C., Schultz, P.G., 2001. Comparative analysis of the immunological evolution of antibody 28B4. Biochemistry 40, 10764–10773.